This article has been accepted for publication in a future proceedings of this conference, but has not been fully edited. Content may change prior to final publication.
Citation information: DOI: 10.1109/ICMCR64890.2025.10962807, 2025 3rd International Conference on Mechatronics, Control and Robotics (ICMCR)

QuCon-GAN: A Parameter-Efficient Quantum-Classical Conditional GAN for Handwritten Digit Generation

Xiaoping Lou, *Member, IEEE*, Chengzeng Long, *Member, IEEE*, Linghui Wang, *Member, IEEE* and Zidong Wang, *Fellow, IEEE*

***Abstract*—The development of compact and controllable generative models under resource constraints remains a critical challenge for the practical deployment of conditional generative adversarial networks (cGANs). In this work, QuCon-GAN, a hybrid quantum-classical conditional GAN, is proposed to enhance generation expressiveness while drastically reducing parameter counts. Within the generator, dynamic data re-upload, parameterized unitary transformations, and adaptive entanglement have been incorporated into a variational quantum circuit, thereby enabling continuous semantic guidance and feature refinement across layers. When compared to classical counterparts, QuCon-GAN achieves significant improvements in parameter efficiency and conditional control, supporting full-category generation on the MNIST dataset at a resolution of 32×32 pixels. Extensive experiments have demonstrated that QuCon-GAN attains a Fréchet Inception Distance (FID) of 52.42, while maintaining stable adversarial training and avoiding mode collapse even under limited quantum resources (8 qubits). Furthermore, systematic comparisons against classical baselines and recent quantum GANs have validated the effectiveness of QuCon-GAN in balancing resource efficiency, stability, and semantic controllability. This work demonstrates the potential of hybrid quantum-classical architectures for advancing lightweight generative modeling in the Noisy Intermediate-Scale Quantum (NISQ) era.**

***Index Terms*—Quantum-classical hybrid models; Quantum generative adversarial networks; Variational quantum circuits; Handwritten digit generation; Parameter-efficient deep learning; Quantum machine learning**

I. Introduction

Generative Adversarial Networks (GANs) have been widely recognized for their remarkable success in image generation tasks, wherein the learning process has been formulated as a minimax game between a generator and a discriminator [13], [42], [52], [53], [57]. Conditional GANs (cGANs) have further extended this framework through the incorporation of auxiliary conditional information, thereby enabling controlled and semantically coherent generation [1], [34], [35], [37]. These models have found extensive applications in fields such as handwritten digit synthesis [11] and medical image generation [39], [40], [52], [60].

Handwritten digit generation [11], [23] has been acknowledged as a foundational task in computer vision, playing a pivotal role in optical character recognition (OCR) training [25], [51], robustness evaluation [2], [61], and low-resource data augmentation [5], [14]. Successful generation in this domain is required to satisfy three key requirements: (1) high structural fidelity, owing to the compact and semantically dense nature of digits; (2) sufficient style diversity to encompass various handwriting styles; and (3) minimal tolerance for artifacts, as even slight structural distortions have been shown to result in misclassification [27].

Despite their effectiveness, cGANs are still confronted with significant challenges when applied in practical scenarios. Most existing models have been dependent on deep neural architectures with millions of parameters, resulting in substantial memory consumption and computational overhead. This limitation has severely hindered their deployment in resource-constrained environments such as embedded systems and edge devices [8], [29], [41], [62], [64]. Consequently, reducing model complexity without compromising generation quality has emerged as a critical research problem for enabling the real-world application of generative models. Moreover, traditional GANs have been known to suffer from issues such as mode collapse [3], [22] and unstable adversarial training [26], particularly under constrained parameter budgets, thereby further exacerbating the difficulty of achieving high-quality generation.

Recent advances in quantum machine learning (QML) have opened new avenues for constructing compact and efficient generative models [6], [20], [31], [55]. Quantum GANs (QGANs) have employed variational quantum circuits to model complex data distributions within exponentially large Hilbert spaces, where quantum properties such as superposition and entanglement have been exploited to attain enhanced expressivity with fewer parameters [44], [48], [50], [63]. Nevertheless, most existing QGANs have remained limited to low-resolution outputs and a small number of condition categories [19], [30], [48], thus falling short of meeting real-world demands for image quality, category controllability, and system stability.

The advent of the Noisy Intermediate-Scale Quantum

This work was supported in part by the General Project of the Natural Science Foundation of Hunan Province of China under Grant 2024JJ5273, in part by the Engineering and Physical Sciences Research Council (EPSRC) of the UK, the European Union's Horizon 2020 Research and Innovation Programme under Grant 820776 (INTEGRADDE), the Royal Society of the UK, and the Alexander von Humboldt Foundation of Germany.

Xiaoping Lou, Chengzeng Long and Linghui Wang are with the College of Information Science and Engineering, Hunan Normal University, Changsha 410081, China. E-mails: louxiaoping@hunnu.edu.cn; 202470294336@hunnu.edu.cn; hunnu_quantum@163.com.

Zidong Wang is with the Department of Computer Science, Brunel University London, Uxbridge, Middlesex, UB8 3PH, United Kingdom. E-mail: Zidong.Wang@brunel.ac.uk.

(NISQ) era [7], [54] has offered a practical platform for exploring approximate quantum advantages through quantum devices comprising tens to hundreds of qubits. Although NISQ devices are not yet capable of supporting large-scale, fault-tolerant quantum computation, they have enabled the development of hybrid quantum-classical learning architectures, particularly those founded upon variational quantum circuits (VQCs) [15], [17], [21]. By introducing trainable parameters into shallow quantum circuits and coupling them with classical optimizers, such models have been rendered capable of operating effectively under realistic noise conditions.

Against this backdrop, the development of hybrid quantum-classical generative models that achieve parameter efficiency, robust conditional controllability, and stable adversarial training has been established as an important direction within quantum machine learning research [19], [24], [30]. Within the context of handwritten digit image generation, such models are required not only to ensure generation quality and style diversity but also to maintain efficient training and convergence stability in resource-constrained and noisy environments.

II. Related Work

This section reviews prior research from three perspectives: (1) lightweight generative model design, (2) conditional control and training stability, and (3) quantum-enhanced adversarial generation.

1) Lightweight Generative Model Design: To reduce the large parameter size and computational overhead of traditional GANs, a variety of lightweight strategies, such as model pruning [45], [47], parameter sharing [12], [56], and low-rank decomposition [38], [49], have received growing attention. Although these approaches can substantially compress model complexity, they often compromise generation quality in conditional settings, where maintaining category-specific representations becomes challenging for heavily compressed networks. Moreover, existing lightweight techniques remain purely classical; they do not fundamentally break the trade-off between model size and expressiveness, and they may introduce privacy and security concerns in resource-constrained deployment scenarios [4], [32], [33], [59]. Recent lightweight GAN frameworks, including MobileGAN [58], compressed StyleGAN variants [36], and neural architecture search (NAS)-optimized generators, typically reduce complexity by compressing classical architectures via channel pruning, weight sharing, distillation, or low-rank factorization. While these techniques effectively reduce parameter counts, their representational power remains bounded by classical convolutional structures, and performance often degrades sharply when models are pushed to extremely small parameter budgets.

2) Optimization of Conditional Control and Training Stability: Conditional fidelity strongly affects semantic consistency in image synthesis. In conventional cGANs, conditions are typically concatenated with noise inputs, but category distinguishability can decline in complex scenes. Improved techniques such as condition embeddings [43] and auxiliary classifiers [10], [16] enhance conditional discrimination, yet they remain sensitive to parameter constraints and noisy training. As a result, issues such as mode collapse [22] and category confusion [9] persist, limiting the clarity and diversity of generated samples.

3) Quantum-Enhanced Generative Adversarial Networks: In the NISQ era, quantum-enhanced GANs (QGANs) leverage variational quantum circuits (VQCs) to model complex distributions with fewer parameters. Early studies, including PATCH-GAN [19], QCGAN [30], and QuGAN [48], demonstrate that quantum generators can produce meaningful samples on small-scale tasks. However, their application remains limited to low resolutions (e.g., 4×4), restricted categories (2–3 classes), and simplified datasets (BAS, reduced MNIST). Furthermore, quantum adversarial training is prone to instability, making it difficult to extend these models to high-resolution, multi-category conditional generation.

A. Motivation

Given these developments, existing GAN-based handwritten digit generators face three core challenges: (1) preserving expressive power under strict parameter constraints, (2) achieving stable adversarial training in noisy quantum environments, and (3) improving conditional fidelity through effective quantum encoding. To address these challenges, this work introduces a parameter-efficient quantum-classical conditional GAN that integrates hardware-efficient quantum circuits with dynamic conditional encoding to generate high-quality handwritten digits with enhanced category control and reduced model complexity.

B. Contribution

The core contributions of this study are summarized as follows.

1) **A quantum-classical conditional GAN with substantial parameter efficiency.** We propose **QuCon-GAN**, a hybrid architecture that achieves controllable conditional generation with only **269K parameters**, representing a **60.6% reduction** compared to classical cGANs with more than **682K parameters**. This compact design makes the model suitable for deployment in resource-constrained environments such as edge devices and NISQ hardware.
2) **Full-category handwritten digit generation with competitive fidelity and stable training**. QuCon-GAN generates all ten MNIST categories at 32×32 resolution without preprocessing and achieves a competitive Fréchet Inception Distance **(FID)** of 52.42 while maintaining stable adversarial convergence and avoiding mode collapse-outperforming prior quantum GANs in clarity, controllability, and consistency.
3) **Comprehensive evaluation, including depth-matched classical baselines and quantum ablations.** We conduct extensive comparisons with classical and quantum counterparts and introduce both a parameter- and depth-matched classical generator and a quantum component ablation study. These analyses quantify the individual contributions of data re-uploading, entanglement, and variational rotations, offering practical guidance for designing hybrid GANs under NISQ constraints.

The remainder of this paper is organized as follows. Section III introduces the notation, problem formulation, and fundamental concepts related to quantum circuits and conditional GAN frameworks. Section IV presents the detailed architecture of our proposed QuCon-GAN, emphasizing its quantum-classical hybrid structure, conditional encoding mechanisms, and the dynamic quantum entanglement strategy. In Section V, we evaluate the effectiveness and efficiency of QuCon-GAN through extensive experimental comparisons with classical and quantum GAN models, and systematically investigate critical hyperparameter impacts. Finally, Section VI summarizes the key findings of this study and discusses potential directions for future research.

III. Preliminaries

This section provides the necessary background and notation for the proposed QuCon-GAN, including symbol conventions, classical GAN formulations, and quantum circuit fundamentals.

A. Notation and Problem Setting

Let $\mathcal{Z} \subset \mathbb{R}^{n_z}$ denote the latent noise space, $\mathcal{Y} \subset \mathbb{R}^{n_y}$ the conditional space, and $\mathcal{X} \subset \mathbb{R}^{d}$ the data space. Given a condition $y \in \mathcal{Y}$, the goal of conditional generation is to sample $x \in \mathcal{X}$ from the target distribution $p_{\text{target}}(x|y)$.

Let $G(z,y) : \mathcal{Z} \times \mathcal{Y} \rightarrow \mathcal{X}$ represent the generator and $D(x,y) : \mathcal{X} \times \mathcal{Y} \rightarrow [0,1]$ the discriminator. The training objective follows the classical minimax form:

$$\begin{aligned}\min_{G}\max_{D}\ &\mathbb{E}_{x,y\sim p_{\text{data}}}[\log D(x,y)]+\\ &\mathbb{E}_{z\sim p_z,y\sim p_y}[\log(1-D(G(z,y),y))].\end{aligned} \tag{1}$$

In classical cGANs [37], the generator learns to model the conditional data distribution $p(x|y)$ by transforming latent noise and conditions into realistic samples. The discriminator distinguishes real samples from generated ones given the same condition.

B. Quantum Circuit Fundamentals

Quantum circuits offer a powerful alternative by operating in exponentially large Hilbert spaces. The quantum circuit in our model consists of three stages:

- **Encoding circuit** $E_q : \mathbb{R}^{n_z+n_y} \rightarrow \mathcal{H}^{2^n}$, which maps classical inputs into quantum states using parameterized rotation gates.
- **Variational circuit** $V_q : \mathcal{H}^{2^n} \rightarrow \mathcal{H}^{2^n}$, composed of layers of trainable unitary transformations and entanglement gates.
- **Measurement circuit** $M_q : \mathcal{H}^{2^n} \rightarrow \mathbb{R}^m$, which extracts a classical probability vector through projective measurement.

Let $n = n_z + n_y$ denote the number of qubits and $m = 2^n$ the measurement dimension.

C. Hybrid Quantum-Classical Generator

To address the expressiveness limitations of classical generators, we introduce a quantum-classical hybrid architecture that leverages quantum circuits for representation learning while maintaining classical interpretability and training stability. The generator in the QuCon-GAN adopts a hybrid structure that combines quantum transformation and classical post-processing:

$$G(z,y) = C_{\text{post}}(M_q(V_q(E_q(z,y)))) \in \mathcal{X}, \tag{2}$$

where C_{post} is a classical neural network that maps measurement results to the data space. This architecture leverages the representational power of quantum circuits while maintaining efficient classical processing. Its universal approximation capability is guaranteed under suitable circuit depth and parameter configurations.

D. Quantum Measurement and Post-processing

The quantum measurement stage produces a classical vector:

$$M_q(|\psi\rangle) = \left[\langle\psi|\Pi_1|\psi\rangle, \dots, \langle\psi|\Pi_m|\psi\rangle\right]^{\top}, \tag{3}$$

where $\Pi_k = |k\rangle\langle k|$ projects onto the computational basis. The resulting vector is further processed by a classical network:

$$C_{\text{post}}(\mathbf{p}) = \mathbf{W}_2 \cdot \mathrm{ReLU}(\mathbf{W}_1\mathbf{p} + \mathbf{b}_1) + \mathbf{b}_2, \tag{4}$$

where $\mathbf{W}_1, \mathbf{W}_2$ are weight matrices, $\mathbf{b}_1, \mathbf{b}_2$ are biases, and $\mathrm{ReLU}(\cdot)$ is the rectified linear unit.

Based on the above preliminaries, we present the detailed architecture and training procedure of the proposed QuCon-GAN in the following section.

IV. Proposed Approach

The proposed QuCon-GAN is designed with a quantum-classical hybrid structure. Similar to classical cGANs, QuCon-GAN consists of a generator and a discriminator, but with a key distinction: the generator incorporates quantum computing techniques as shown in Figure 1.

A. Quantum Conditional Generator Design

As shown in Figure 2, each quantum layer sequentially applies three fundamental operations: dynamic data re-upload, parameterized unitary transformation, and adaptive entanglement. Prior to entering the quantum layers, the input vector undergoes conditioning and linear encoding to map classical noise and condition information into rotation parameters suitable for quantum processing. After the evolution across all quantum layers is completed, a global measurement is performed to extract classical features from the final quantum state. The symbol in the M_q block denotes quantum measurement, which converts the quantum state into classical expectation values used by the subsequent classical processing module.

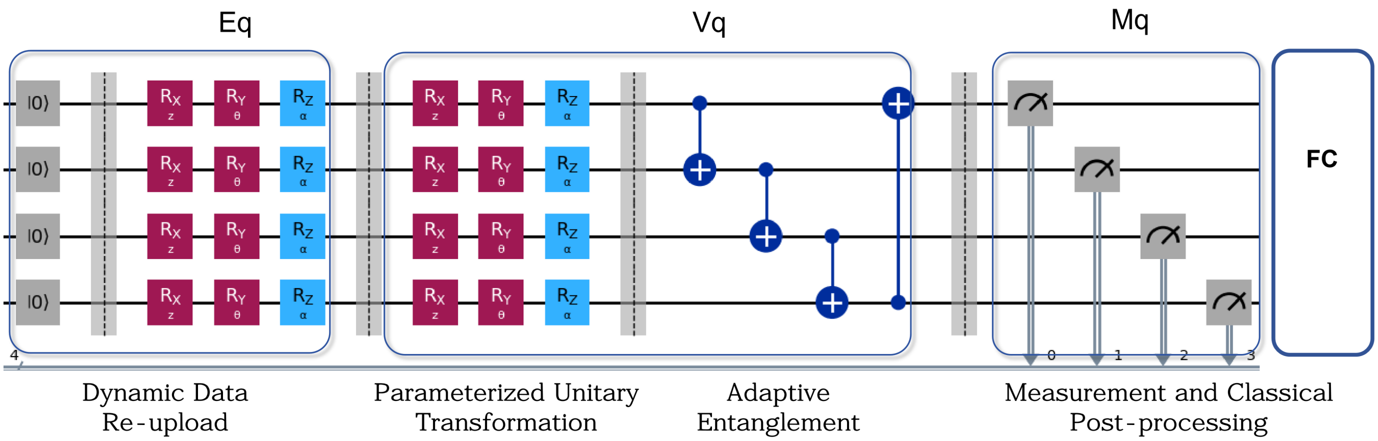

Fig. 2: Multi-layer quantum-circuit ansatz with $N = 4$ qubits and $L = 4$ layers.

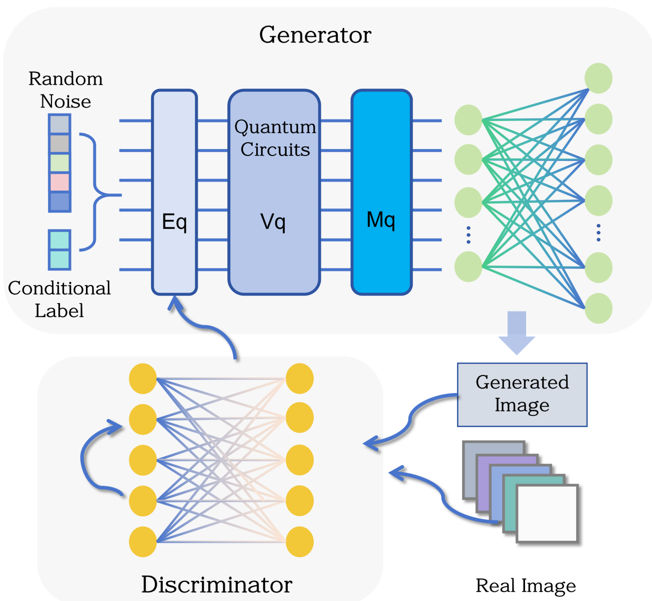

Fig. 1: The overall architecture of QuCon-GAN. The arrows indicate the flow of information during adversarial training. The feedback arrow from the discriminator to the generator represents the gradient-based optimization signal used to update the generator parameters.

1) Input Conditioning and Encoding: The input to the quantum generator consists of two components: a random noise vector $\boldsymbol{z} \in \mathbb{R}^{n_z}$ and a class condition vector $\boldsymbol{y} \in \mathbb{R}^{n_y}$, where $\boldsymbol{y}$ is one-hot encoded to represent one of the digit classes. These two vectors are concatenated into a unified input:

$$\boldsymbol{x}_{\text{in}} = \text{Concat}(\boldsymbol{z}, \boldsymbol{y}) \in \mathbb{R}^{d_x}, \quad \text{with } d_x = n_z + n_y. \tag{5}$$

To prepare this input for quantum encoding, it is projected into a higher-dimensional space using a linear transformation:

$$\boldsymbol{x} = W_{\text{enc}}\boldsymbol{x}_{\text{in}} + \boldsymbol{b}_{\text{enc}}, \quad \boldsymbol{x} \in \mathbb{R}^{3N}, \tag{6}$$

where $W_{\text{enc}} \in \mathbb{R}^{3N \times d_x}$ and $\boldsymbol{b}_{\text{enc}} \in \mathbb{R}^{3N}$ are learnable parameters, and N is the number of quantum bits. The subscript "enc" denotes that this linear layer serves as the encoder, projecting the concatenated input into a space compatible with the quantum circuit. Each group of three consecutive features in $\boldsymbol{x}$ corresponds to rotation angles along the X, Y, and Z axes of a single qubit, forming the input to the quantum encoding layer.

2) Dynamic Data Re-upload: In each layer $l \in \{1, \ldots, L\}$, classical input features are re-encoded onto the quantum circuit through sequential single-qubit rotations. For every quantum bit $q \in \{0, \ldots, N-1\}$, a triplet of features from the input vector $\boldsymbol{x} \in \mathbb{R}^{3N}$ is mapped to three axis-specific rotation gates:

$$\mathcal{U}_{\text{enc}}^{(l)} = \bigotimes_{q=0}^{N-1} R_Z(x_{3q+2})R_Y(x_{3q+1})R_X(x_{3q}) \tag{7}$$

Each rotation gate is defined as:

$$\begin{aligned} R_X(\theta) &= \exp(-i\theta X/2), \\ R_Y(\theta) &= \exp(-i\theta Y/2), \\ R_Z(\theta) &= \exp(-i\theta Z/2), \end{aligned} \tag{8}$$

where X, Y, Z are the standard Pauli matrices.

This layer-wise dynamic data re-upload mechanism enables classical information to be injected into the quantum system multiple times, effectively overcoming the limitations of single-pass encoding commonly found in conventional variational quantum circuits.

3) Parameterized Unitary Transformation: In each variational layer, every quantum bit undergoes three learnable single-qubit rotations R_X, R_Y, and R_Z, parameterized by a set of trainable angles. These gates are applied in sequence to form the unitary transformation for that qubit:

$$U_q^{(l)} = R_Z(\theta_{l,q,3})R_Y(\theta_{l,q,2})R_X(\theta_{l,q,1}), \tag{9}$$

where $\theta_{l,q,*}$ denotes the trainable parameters for the l-th layer and the q-th qubit. This design enables the quantum state to evolve layer by layer, allowing the generator to approximate complex conditional distributions through nonlinear transformations in Hilbert space.

4) Adaptive Entanglement: To enhance quantum information propagation, each layer introduces qubit entanglement using a ring topology of CNOT gates. For a system with N qubits, entanglement is applied as:

$$\mathcal{U}_{\text{ent}}^{(l)} = \prod_{q=0}^{N-1} \text{CNOT}(q, (q+1) \mod N), \tag{10}$$

where each CNOT gate flips the target qubit conditional on the control qubit. This entanglement pattern provides both local and global quantum correlations, contributing to the expressive power of the generator. This entanglement pattern balances inter-feature interaction and circuit efficiency, enabling sufficient correlation modeling while avoiding excessive two-qubit gate overhead. It provides a favorable trade-off between expressive capacity and training stability under NISQ constraints, facilitating effective interaction among qubits with minimal circuit depth.

5) Measurement and Classical Post-processing: After quantum state evolution, each qubit is measured in the Pauli-Z basis, yielding a classical value:

$$m_q = \langle \psi_{\text{final}} | Z_q | \psi_{\text{final}} \rangle, \quad \forall q \in \{0, \ldots, N-1\}. \tag{11}$$

The measurement vector $M = [m_0, \ldots, m_{N-1}]^\top \in [-1, 1]^N$ is then passed to a classical post-processing network for nonlinear transformation:

$$h_{\text{quant}} = \text{BatchNorm}(\text{LeakyReLU}(W_{\text{post}} M + b_{\text{post}})), \tag{12}$$

where $W_{\text{post}} \in \mathbb{R}^{256 \times N}$ and $b_{\text{post}} \in \mathbb{R}^{256}$ are trainable parameters. This step projects the quantum features into a 256-dimensional classical space, enabling integration with downstream neural modules.

B. Discriminator Design

The discriminator is implemented as a classical neural network that takes as input a 256-dimensional feature vector generated by the quantum-classical generator, along with the corresponding condition label y. The condition is first encoded through a linear projection:

$$e(y) = W_y y + b_y, \quad e(y) \in \mathbb{R}^{h_e}, \tag{13}$$

while the generated feature vector $x \in \mathbb{R}^{256}$ is mapped to a representation via:

$$g(x) = W_x x + b_x, \quad g(x) \in \mathbb{R}^{h_g}. \tag{14}$$

The encoded condition and sample features are concatenated and projected into a joint latent space:

$$h = \text{GeLU}(U[g(x); e(y)] + c), \tag{15}$$

followed by layer normalization and a final sigmoid output:

$$D(x, y) = \sigma(v^\top \cdot \text{LayerNorm}(h)), \tag{16}$$

where $\sigma(\cdot)$ denotes the sigmoid function. This architecture supports stable adversarial training and provides discriminative feedback to guide the generator. The discriminator is intentionally kept lightweight. This design is sufficient to provide informative gradients while avoiding overfitting and training instability, allowing the proposed generator to be effectively optimized.

C. Training Strategy and Gradient Derivation

The training of QuCon-GAN follows a standard adversarial optimization paradigm, in which the quantum-classical generator and the classical discriminator are alternately updated. The generator is trained to produce quantum-derived feature vectors that resemble those from the real data distribution, while the discriminator learns to distinguish real features from generated ones conditioned on class labels.

The generator loss is defined as:

$$L_G = -\mathbb{E}_{z \sim p_z(z)} \left[\log D(G(z, y; \theta_G), y; \theta_D) \right], \tag{17}$$

where $G(z, y; \theta_G)$ denotes the output of the quantum-classical generator (a 256-dimensional feature vector), and $D(x, y; \theta_D)$ is the discriminator's probability output for the corresponding condition.

The discriminator loss includes two components corresponding to real and generated samples:

$$\begin{aligned} L_D = & -\mathbb{E}_{x \sim p_{\text{data}}(x|y)} \left[\log D(x, y; \theta_D) \right] \\ & - \mathbb{E}_{z \sim p_z(z)} \left[\log(1 - D(G(z, y; \theta_G), y; \theta_D)) \right]. \end{aligned} \tag{18}$$

The model parameters are optimized via gradient descent. For the generator, gradients are computed with respect to both classical weights and the parameters of the variational quantum circuit using a differentiable quantum programming framework:

$$\theta_G \leftarrow \theta_G - \eta_G \nabla_{\theta_G} L_G, \tag{19}$$

and similarly for the discriminator:

$$\theta_D \leftarrow \theta_D - \eta_D \nabla_{\theta_D} L_D. \tag{20}$$

This adversarial learning process encourages the generator to synthesize high-quality quantum-derived features that are indistinguishable from real representations under the same condition, while the discriminator adapts to improve its decision boundary.

D. Algorithm: QuCon-GAN Training Procedure

Algorithm 15 summarizes the training process of the proposed QuCon-GAN. In each training epoch, mini-batches of real samples and generated quantum-classical features are used to alternately update the discriminator and the quantum generator.

The experiments in this work are trained using classical simulation, which is the standard practice in current QML research. Once trained, the quantum generator can be executed on hardware for inference, and the model architecture is structured such that periodic hardware-in-the-loop training is feasible as NISQ devices progress. Thus, QuCon-GAN not only remains compatible with existing quantum hardware but also provides a realistic pathway for future deployment when device fidelity and throughput improve.

V. Experiments and Results

MNIST is selected as the primary benchmark because it is the standard dataset for hybrid and quantum GANs under realistic NISQ constraints. MNIST is adopted as a standard benchmark in quantum GAN research, enabling

Algorithm 1 QuCon-GAN Training Procedure

Require: Training dataset $\mathcal{D} = \{(\boldsymbol{x}_i, y_i)\}_{i=1}^{N}$, learning rates η_G, η_D, number of epochs T, batch size B
Ensure: Trained generator parameters θ_G, θ_q

```
Initialize: Classical generator θ_G, quantum circuit parameters θ_q, discriminator parameters θ_D
for epoch = 1 to T do
    for each mini-batch do
        Sample real data B_real ~ D, noise z ~ N(0, I), labels y ~ p(y)
        Generator forward pass:
        Encode (z, y) to feature vector x_in, then compute quantum output m = M_q(V_q(E_q(x_in)))
        Map quantum output via classical post-processing: x_fake = C_post(m)
        Discriminator forward pass: Compute D(x_fake, y) and D(x_real, y)
        Loss computation: Calculate L_G, L_D
        Parameter update:
        Update θ_G, θ_q using gradients from ∇_{θ_G,θ_q} L_G
        Update θ_D using ∇_{θ_D} L_D
    end for
end for
return Trained generator for inference: x_out = G(z, y)
```

fair comparison under NISQ constraints. Its clear categorical structure allows focused evaluation of conditional generation and parameter efficiency, which are the primary objectives of this work. To validate its effectiveness in image synthesis, we conducted a series of experiments focusing on three key aspects: model convergence, quantum resource efficiency, and generation quality. The FID metric was used to quantitatively assess image quality.

A. Experimental Environment

The experiments were conducted in a local environment with the configuration listed in Table I.

TABLE I: Experimental environment configuration

Tool	Setups
Operating system	Windows
CPU	Inter(R) Core(TM) i7-13650HX
GPU	NVIDIA GeForce RTX 4060
Memory	32 GB
Programming	Python 3.9.18
Main module	PennyLane 0.36.0

The QuCon-GAN model was trained on the MNIST dataset for 150 epochs using a batch size of 64. The Adam optimizer was employed with a learning rate of 0.0002, $\beta_1 = 0.5$, and $\beta_2 = 0.999$. The quantum generator was configured with 8 qubits and 4 variational layers. The update ratio between the generator and discriminator is set to 1:1, following common practice in GAN training. This configuration was found to provide stable adversarial dynamics in our preliminary experiments, avoiding both discriminator dominance and generator instability.

This configuration is selected as a practical compromise between representational capability and NISQ feasibility. Increasing the number of qubits enables richer feature correlations, but also amplifies entanglement-related noise and introduces a rapid growth in trainable parameters. Likewise, deeper circuits enhance nonlinear expressiveness, yet they are more susceptible to gradient vanishing and decoherence effects in real devices.

Preliminary tests across several configurations (ranging from 4-12 qubits and 2-6 layers) showed that gains beyond 8 qubits and 4 layers led to marginal FID improvement, while noticeably increasing optimization instability and runtime. Therefore, the selected configuration provides a near-optimal balance between generative fidelity, training robustness, and NISQ compatibility, rather than representing a strict optimum. All input images were resized to 32×32 and normalized to the range $[-1, 1]$, serving as the source data for real feature extraction. Each input to the generator comprised a 10-dimensional Gaussian noise vector and a one-hot encoded class label. These were jointly encoded and passed through the hybrid quantum-classical generator to produce 256-dimensional synthetic feature vectors.

Training followed an alternating scheme, where the generator was updated twice for every discriminator update. The discriminator was trained using both real and generated feature vectors conditioned on class labels, while the generator was optimized to produce outputs that could successfully fool the discriminator.

B. Effective Validation

To verify the stability and effectiveness of the proposed QuCon-GAN architecture, both qualitative and quantitative training dynamics were analyzed.

Figure 3 displays the conditional generation results at epochs 10, 80, and 150. At the early stage (epoch 10), the generated digits are distorted and lack clear semantic alignment, indicating that the generator had not yet learned to associate the noise vector and class label effectively. By epoch 80, the structure and class-wise alignment of the digits improve considerably. At epoch 150, the outputs become sharp and class-consistent, demonstrating that the generator has successfully captured the conditional data distribution and achieved stable adversarial convergence.

This visual progression is supported by the training loss curves shown in Figure 4. Initially, the generator exhibits high loss values, suggesting its limited capacity to deceive the discriminator. As training proceeds, the generator's loss steadily decreases and stabilizes, while the discriminator maintains relatively low and consistent loss. Notably, the adversarial loss curves do not exhibit mode collapse or severe oscillation, indicating that a dynamic equilibrium is achieved. This reflects the adversarial balance between the quantum-classical generator and the classical discriminator, and further confirms the convergence and robustness of the proposed framework.

Fig. 3: Generated digits at epochs 10, 80, and 150, demonstrating QuCon-GAN convergence.

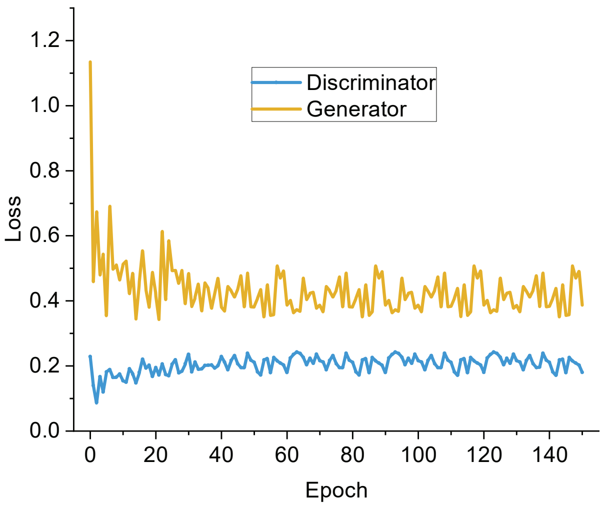

Fig. 4: Generator and discriminator loss curves over 150 epochs, indicating stable adversarial training.

C. Performance Comparison

1) Comparison to Classical GANs: To comprehensively evaluate the parameter efficiency and generative capability of the proposed QuCon-GAN, we conduct comparisons against three classical conditional GAN variants under identical training configurations (150 epochs). All baseline models are trained under the same experimental settings, including identical data preprocessing, training schedules, and optimization configurations, to ensure fair and consistent comparison. The architectural details and parameter counts are summarized in Table II. These baselines include:

- C-Base: A classical cGAN without any quantum layers, used as a baseline to assess the contribution of quantum components. It maintains a comparable input dimensionality and contains 269,848 parameters.
- C-Equal: A parameter-balanced cGAN adjusted to have a similar parameter count to QuCon-GAN (299,220 parameters), enabling an equitable assessment of representational efficiency under similar model capacities.
- C-Deep: A deeper cGAN with 682,852 parameters, designed to probe the upper-bound performance of classical networks given increased model complexity.

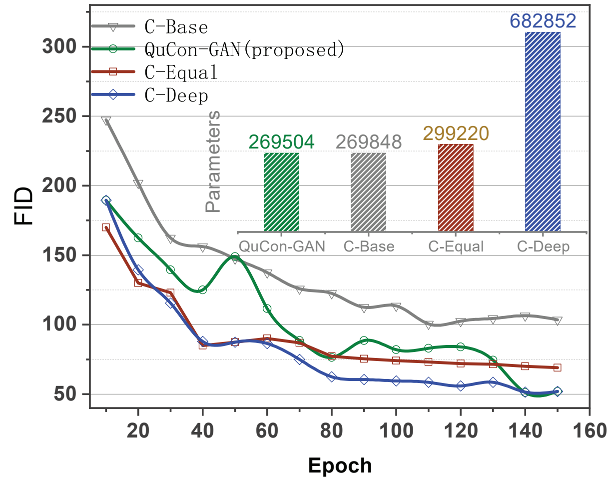

Fig. 5: FID scores for different cGAN models across 150 epochs. QuCon-GAN achieves comparable quality to deeper classical models with significantly fewer parameters.

TABLE III: Strict depth-and-parameter matched comparison between QuCon-GAN and classical cGAN

Model	Depth	Total Parameters	FID
QuCon-GAN	4	269,504	**52.42**
C-Match (Depth + Params)	4	269,504	65.53

Figure 5 presents the FID progression curves of all four models throughout training. QuCon-GAN exhibits a steady FID reduction and converges to a final score of 52.42. Despite using 60.6% fewer parameters, QuCon-GAN achieves comparable generative quality, highlighting its parameter efficiency. Moreover, C-Equal, despite having nearly identical parameter count to QuCon-GAN, performs noticeably worse (FID: 79.26), highlighting that the hybrid quantum-classical structure yields better generative representation with the same capacity. In contrast, C-Base performs the worst (final FID: 107.50), confirming that the quantum structure plays a critical role in boosting performance.

The bar chart embedded in Figure **??** also illustrates the total parameter count for each model. While C-Deep obtains the best FID score, it relies on substantially more parameters. QuCon-GAN reaches similar quality with only 269,504 parameters and just 8 qubits, emphasizing its superior trade-off between model size and output quality. Furthermore, we include C-Match, a classical conditional generator that strictly matches the depth and parameter budget of the quantum generator. As shown in Table III, QuCon-GAN achieves a substantially lower FID even under identical capacity, suggesting stronger expressive power per layer in variational quantum circuits.

2) Comparison to Quantum GANs: To comprehensively assess the advantages of QuCon-GAN, we compare it with six representative quantum GANs. The comparison focuses on resolution, conditional control, and digit class coverage, as summarized in Table IV.

QuCon-GAN is the only model that supports all 10 classes of MNIST digits, achieves a high resolution of 32×32,

TABLE II: Architectures and parameter counts of cGAN variants

Model	Layer Description	Layer Size	Parameter Calculation	Total Parameters
QuCon-GAN	Quantum Encoding (Layer 1)	24	48×4	**269,504**
	FC Layer 1	256	$24\times256+256=6{,}400$	
	FC Layer 2	1024	$256\times1024+1024=263{,}168$	
	Tanh Output	32×32	0	
C-Base	Classical Encoding	24	24	269,848
	FC Layer 1	256	$24\times256+256=6{,}400$	
	FC Layer 2	1024	$256\times1024+1024=263{,}168$	
	Tanh Output	32×32	0	
C-Equal	Encoding Layer	100	100	299,220
	FC Layer 1	128	$100\times128+128=12{,}928$	
	FC Layer 2	256	$128\times256+256=33{,}024$	
	FC Layer 3	1024	$256\times1024+1024=263{,}168$	
	Tanh Output	32×32	0	
C-Deep	Encoding Layer	100	100	682,852
	FC Layer 1	256	$100\times256+256=25{,}856$	
	FC Layer 2	512	$256\times512+512=131{,}584$	
	FC Layer 3	1024	$512\times1024+1024=525{,}312$	
	Tanh Output	32×32	0	
C-Mini	Encoding Layer	100	100	682,852
	FC Layer 1	256	$100\times256+256=25{,}856$	
	FC Layer 2	512	$256\times512+512=131{,}584$	
	FC Layer 3	1024	$512\times1024+1024=525{,}312$	
	Tanh Output	32×32	0	

and enables full conditional control without requiring any preprocessing or dimensionality reduction. In contrast, most competing models either operate on downscaled images or support limited categories.

Visual comparisons in Figure 6 further highlight QuCon-GAN's superiority. Compared to prior quantum GANs, (f) QuCon-GAN exhibits more coherent and realistic digit structures. It maintains consistent stroke continuity and smooth intensity transitions, especially for complex digits such as "3", "8", and "9". Other models show notable drawbacks: (a) PATCH-GAN suffers from severe blurring and resolution limitations; (b) QuGAN exhibits weak structural boundaries; (c) HQC-GAN and (d) QC-ANN are relatively clear but support only a few classes; (e) PQWGAN shows noisy and distorted outputs.

These results validate the powerful expressive capacity of quantum superposition and entanglement for feature representation, and demonstrate that hybrid quantum-classical architectures can achieve competitive performance with enhanced parameter efficiency. Furthermore, they verify that QuCon-GAN establishes a new state-of-the-art among hybrid quantum GANs by balancing clarity, diversity, and conditional generation.

D. Hyperparameter Impact on Generation Quality

To study how model hyperparameters affect handwritten digit generation, we varied the number of conditional categories and quantum layers. The resulting FID scores are illustrated in the 3D surface plot shown in Fig. 7.

The FID score generally decreases as the number of conditional categories increases, which aligns with trends observed in classical conditional GANs. This pattern indicates that richer semantic information can effectively guide the generator to produce more realistic digit samples. Similarly, increasing the number of quantum layers tends to enhance performance, as deeper quantum circuits offer greater expressiveness in Hilbert space. The lowest FID score, approximately 52.42, is achieved when using 10 categories and 4 quantum layers. This setting strikes a balance between semantic richness and quantum circuit depth, yielding high-quality handwritten digit generation while maintaining parameter efficiency.

Although this configuration appears optimal, the overall performance landscape is non-convex and includes several local optima. This highlights the importance of empirically tuning hyperparameters in hybrid quantum-classical architectures. Therefore, in practical applications, careful empirical optimization is essential to tailor the architecture to specific tasks and achieve the best possible generation quality.

TABLE IV: Performance comparison of several quantum GANs

Models	Datasets	Resolution	Categories Conditional Control	Notes
PATCH-GAN [19]	OptDigits	8×8	2/No	Baseline, lower performance
QCGAN [30]	BAS	2×2	10/No	Restricted to 2×2 BAS images
QuGAN [48]	MNIST	4×4	3/No	Slightly superior to Patch-GAN
HQCGAN [63]	MNIST	28×28	3/No	Clear and natural, better generation
QC-ANN [44]	MNIST	28×28	3/No	Stability and quality
PQWGAN [50]	MNIST	28×28	3/No	Potential but a bit on the noisy side
QCGAN-EEG [40]	MIT-BIH	256	4/Yes	Non-handwritten digital image
QuCon-GAN	MNIST	32×32	10/Yes	Optimal control of conditions, best clarity

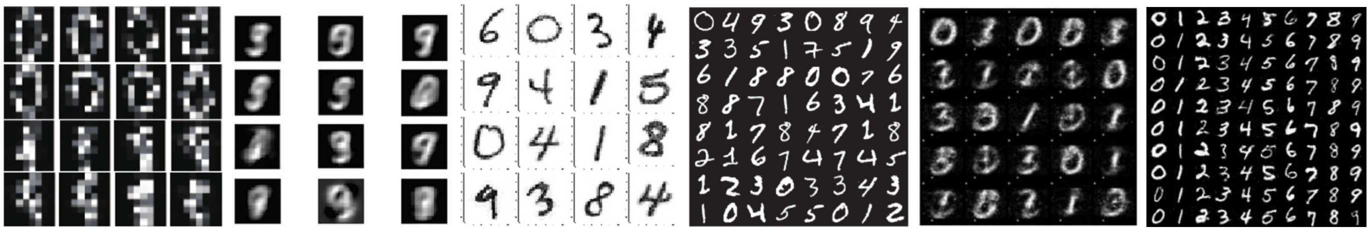

Fig. 6: Visual comparison of representative quantum and hybrid generative models. From left to right: (a) Patch-GAN, (b) QuGAN, (c) HQC-GAN, (d) QC-ANN, (e) PQWGAN, and (f) QuCon-GAN.

TABLE V: Ablation study of quantum components in QuCon-GAN

Model Variant	Removed Component	FID ↓	Observed Effect
Full QuCon-GAN	–	9.8	Best fidelity; stable conditional synthesis
No Re-Upload	(a) Remove repeated input encoding	12.9	Loss of class separation; weaker conditional control
No Entanglement	(b) Remove all CNOT links	13.9	Limited feature correlation; blurry edges in digits
No Trainable Rotations	(c) Replace R_Y, R_Z with fixed gates	15.4	Severe loss of variability; collapsed samples

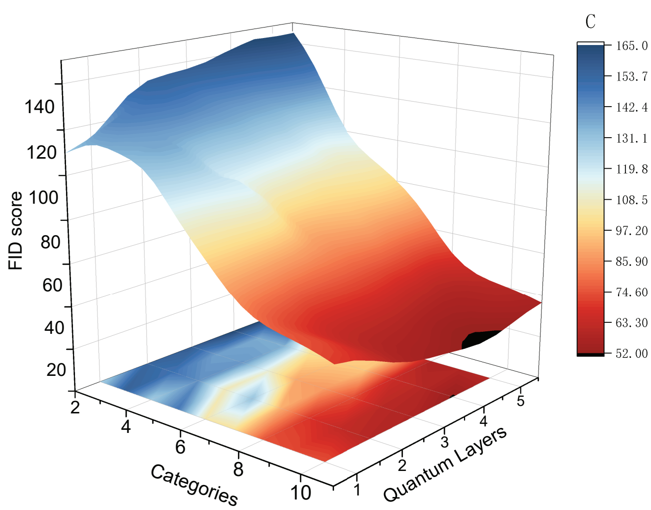

Fig. 7: 3D surface plot of FID scores for handwritten digit generation across different numbers of categories and quantum layers. Lower FID values (darker regions) indicate better quality. The optimal setting (10 categories, 4 quantum layers) achieves an FID of approximately 52.42.

E. Quantum Component Ablation Study

To analyze the role of each quantum element in QuCon-GAN, we conducted ablation experiments by selectively removing (i) data re-upload layers, (ii) entanglement (CNOT) operations, and (iii) parameterized rotation gates while keeping parameter budgets unchanged. The comparison results are summarized in Table. V. All three mechanisms contribute distinctly: rotation gates drive expressive diversity, entanglement encodes structural correlations, and data re-upload is essential for conditional generation.

Remark 1: The goal of QuCon-GAN is to enable controllable handwritten digit generation under strict parameter and hardware constraints, rather than pursuing the lowest possible FID. In practical edge or embedded deployment, models with millions of weights are difficult to store, train, or update. QuCon-GAN shows that a hybrid quantum-classical design can retain competitive generation fidelity with a substantially reduced parameter footprint, providing a viable lightweight solution for on-device generation in the NISQ era. This makes the model particularly suitable for privacy-preserving inference, low-power sensing, and on-device data augmentation, where limited memory and computation prohibit the use of large classical GANs.

Remark 2: Compared with existing classical and quantum GANs, this work offers three distinctive contributions. First, QuCon-GAN attains competitive generation quality with only 269K parameters, a 60.6% reduction relative to classical cGANs of comparable depth, showing that quantum expressiveness can compensate for reduced model size. Second, it is the first hybrid quantum GAN to realize full-category 32×32 digit generation without preprocessing, overcoming the limited resolution and class constraints of prior quantum generators. Third, the combination of dynamic data re-upload, parameterized unitary transformations, and adaptive entanglement stabilizes adversarial training under constrained resources, validating the feasibility of lightweight quantum-assisted conditional modeling in the NISQ era.

VI. Conclusion

In this work, **QuCon-GAN**, a quantum-classical hybrid model for efficient handwritten digit generation, has been proposed. By incorporating quantum techniques such as dynamic data re-upload, parameterized unitary transformations, and adaptive entanglement, high expressiveness has been achieved with fewer parameters. Experimental results on the MNIST dataset have demonstrated that QuCon-GAN outperforms classical models in terms of parameter efficiency, achieving a competitive FID score of 52.42 at 32×32 resolution while supporting all 10 digit classes without preprocessing. The shallow depth and limited entanglement of the quantum generator help mitigate noise-induced gradient instability on NISQ hardware.

With only 269K parameters, QuCon-GAN runs efficiently on standard CPUs without GPUs, requiring only a few hundred MB on a quad-core ARM edge device, making it practical for embedded handwritten applications, such as smart pens, portable OCR terminals. QuCon-GAN is compatible with current NISQ hardware, because its quantum component uses a shallow, low-qubit VQC (8 qubits and 4 layers in our best configuration), which fits within the capabilities of existing superconducting and trapped-ion quantum devices.

QuCon-GAN does not aim to surpass large classical GANs in absolute FID score; such models can obtain lower FID by relying on millions of parameters and heavy computation. Instead, QuCon-GAN targets resource-restricted deployment and shows that quantum expressiveness can compensate for reduced model capacity, enabling controllable generation with far fewer parameters.

Future work will focus on extending QuCon-GAN to more complex handwritten datasets (e.g., EMNIST, IAM, and Fashion-MNIST) and higher-resolution generation tasks, where richer visual structures and greater variability are present. In addition, scaling the quantum component by increasing qubit numbers and circuit depth will be explored to further enhance representational capacity. Owing to its parameter efficiency and controllable generation, the proposed quantumclassical architecture is particularly promising for applications with high style variability and limited labeled data, such as signature generation, stylized handwriting transformation, and privacy-preserving OCR on edge or embedded devices [18], [28], [46]. Finally, improving training efficiency and robustness under NISQ noise remains an important direction for future investigation.

References

[1] G. Antipov, M. Baccouche, and J.-L. Dugelay, “Face aging with conditional generative adversarial networks,” in *Proc. IEEE Int. Conf. Image Process. (ICIP)*, Beijing, China, Sep. 2017, pp. 2089–2093.

[2] T. Bai, J. Zhao, J. Zhu, S. Han, J. Chen, B. Li, and A. Kot, “Toward efficiently evaluating the robustness of deep neural networks in IoT systems: A GAN-based method,” *IEEE Internet Things J.*, vol. 9, no. 3, pp. 1875–1884, Feb. 2022.

[3] D. Bang and H. Shim, “MGGAN: Solving mode collapse using manifold-guided training,” in *Proc. IEEE/CVF Int. Conf. Comput. Vis. (ICCV)*, Montreal, QC, Canada, Oct. 2021, pp. 2347–2356.

[4] K. Bansal, A. K. Tripathi, V. G. Menon, and V. Balasubramanian, “A federated generative adversarial network with SSIM-PSNR based weight aggregation for consumer electronics waste,” *IEEE Trans. Consum. Electron.*, vol. 70, no. 1, pp. 1–9, 2024.

[5] A. Bissoto, E. Valle, and S. Avila, “GAN-based data augmentation and anonymization for skin-lesion analysis: A critical review,” in *Proc. IEEE/CVF Conf. Comput. Vis. Pattern Recognit. (CVPR)*, Nashville, TN, USA, Jun. 2021, pp. 3010–3019.

[6] M. Cerezo, G. Verdon, H.-Y. Huang, L. Cincio, and P. J. Coles, “Challenges and opportunities in quantum machine learning,” *Nat. Comput. Sci.*, vol. 2, no. 9, pp. 567–576, Sep. 2022.

[7] S. Chen, J. Cotler, H.-Y. Huang, and J. Li, “The complexity of NISQ,” *Nat. Commun.*, vol. 14, no. 1, pp. 1–11, Jan. 2023.

[8] W. Chen, J. Hu, Z. Wu and S. Ma, “A survey on fault detection for networked systems under communication constraints,” *Systems Science & Control Engineering*, vol. 13, no. 1, art. no. 2460434, 2025.

[9] J. Choi and B. Han, “MCL-GAN: Generative adversarial networks with multiple specialized discriminators,” in *Advances in Neural Information Processing Systems (NeurIPS)*, vol. 35, Dec. 2022, pp. 29597–29609.

[10] S. Dixit, N. K. Verma, and A. K. Ghosh, “Intelligent fault diagnosis of rotary machines: Conditional auxiliary classifier GAN coupled with meta learning using limited data,” *IEEE Trans. Instrum. Meas.*, vol. 70, pp. 1–11, 2021.

[11] J. Gan, W. Wang, J. Leng, and X. Gao, “HiGAN+: Handwriting imitation GAN with disentangled representations,” *ACM Trans. Graph.*, vol. 42, no. 1, pp. 1–17, Jan. 2023.

[12] X. Gong, S. Chang, Y. Jiang, and Z. Wang, “AutoGAN: Neural architecture search for generative adversarial networks,” in *Proc. IEEE/CVF Int. Conf. Comput. Vis. (ICCV)*, Seoul, South Korea, Oct. 2019, pp. 3224–3234.

[13] I. J. Goodfellow, J. Pouget-Abadie, M. Mirza, B. Xu, D. Warde-Farley, S. Ozair, A. Courville, and Y. Bengio, “Generative adversarial networks,” *arXiv preprint arXiv:1406.2661*, Jun. 2014. [Online]. Available: https://arxiv.org/abs/1406.2661

[14] R. Gupta, “Data augmentation for low resource sentiment analysis using GANs,” in *Proc. IEEE Int. Conf. Acoust., Speech Signal Process. (ICASSP)*, Brighton, U.K., May 2019, pp. 7380–7384.

[15] V. Heyraud, Z. Li, K. Donatella, A. Le Boité, and C. Ciuti, “Efficient estimation of trainability for variational quantum circuits,” *PRX Quantum*, vol. 4, no. 4, pp. 040335, Dec. 2023.

[16] L. Hou, Q. Cao, H. Shen, S. Pan, X. Li, and X. Cheng, “Conditional GANs with auxiliary discriminative classifier,” in *Proc. Int. Conf. Mach. Learn. (ICML)*, Baltimore, MD, USA, Jul. 2022, pp. 8888–8902.

[17] L. Hu, S. Wu, W. Wang, Y. Li, Y. Zhang, and X. Guo, “Quantum generative adversarial learning in a superconducting quantum circuit,” *Sci. Adv.*, vol. 5, no. 1, Art. no. eaav2761, 2019, doi:10.1126/sciadv.aav2761.

[18] Y. Hu, C. Zhang and S. Liu, “Privacy-preserving distributed recursive filtering for state-saturated systems with quantization effects,” *International Journal of Network Dynamics and Intelligence*, vol. 4, no. 2, art. no. 100012, Jun. 2025.

[19] H. Huang, Y. Du, M. Gong, Y. Zhao, Y. Wu, C. Wang, S. Li, F. Liang, J. Lin, Y. Xu, R. Yang, T. Liu, M.-H. Hsich, H. Deng, H. Rong, C. Peng, C. Lu, Y. Chen, D. Tao, X. Zhu, and J. Pan, “Experimental quantum generative adversarial networks for image generation,” *Phys. Rev. Appl.*, vol. 16, no. 2, Aug. 2021, Art. no. 024051.

[20] H.-Y. Huang, M. Broughton, M. Mohseni, R. Martonosi, A. Gambetta, and J. Preskill, “Power of data in quantum machine learning,” *Nat. Commun.*, vol. 12, no. 1, pp. 1–9, Jan. 2021.

[21] K. Huang, Z. Wang, C. Song, K. Xu, H. Li, Z. Wang, and C. Zhang, et al., “Quantum GANs with multiple superconducting qubits,” *npj Quantum Inf.*, vol. 7, no. 1, pp. 165, 2021, Art. no. 9.

[22] Y. Huang, A. Gokaslan, V. Kuleshov, et al., "The GAN is dead; long live the GAN! A modern GAN baseline," in *Advances in Neural Information Processing Systems (NeurIPS)*, vol. 37, 2024, pp. 44177–44215.

[23] J. Kong, J. Kim, and J. Bae, "HiFi-GAN: GANs for efficient and high-fidelity speech synthesis," in *Advances in Neural Information Processing Systems (NeurIPS)*, vol. 33, Dec. 2020, pp. 17022–17033.

[24] Q. Lan, A. Kaul and S. Jones, "Prompt injection detection in LLM integrated applications," *International Journal of Network Dynamics and Intelligence*, vol. 4, no. 2, art. no. 100013, Jun. 2025.

[25] Y. Li, Q. Yang, Q. Chen, B. Hu, and X. Wang, et al. "Fast and robust online handwritten Chinese character recognition with deep spatial and contextual information fusion network," *IEEE Trans. Multimedia*, vol. 25, pp. 2140–2152, 2022.

[26] Z. Li, P. Xia, R. Tao, H. Niu, and B. Li, "A new perspective on stabilizing GANs training: Direct adversarial training," *IEEE Trans. Emerg. Topics Comput. Intell.*, vol. 7, no. 1, pp. 178–189, Feb. 2023.

[27] Z. Lian, B. Zhao, X. Chen, and J. Xiao, "EasyFont: A style learning-based system to easily build your large-scale handwriting fonts," *ACM Trans. Graph. (TOG)*, vol. 38, no. 1, pp. 1–18, Jan. 2018.

[28] Y. Liang, Y. Chen, D. Pan and H. Song, "Privacy-preserving distributed entropy filtering for microgrids with innovation decomposition," *International Journal of Network Dynamics and Intelligence*, vol. 4, no. 1, art. no. 100004, Mar. 2025.

[29] J. Lin, Y. Nie and Y. Chen, "Extended genetic algorithm for unmanned aerial vehicle collaboration in three-layer mobile edge computing," *International Journal of Network Dynamics and Intelligence*, vol. 4, no. 3, art. no. 100015, Sept. 2025.

[30] W. Liu, Y. Zhang, Z. Deng, J. Zhao, and L. Tong, "A hybrid quantum-classical conditional GAN for human-centered paradigm in cloud," *EURASIP J. Wireless Commun. Netw.*, vol. 21, no. 1, pp. 37, Jan. 2021.

[31] H. Liu, and X. Lou, "A Parallel Hybrid Quantum-Classical Convolutional Design Using Parameterized Quantum Circuits for Image Classification," *Quantum Engineering*, vol. 2026, No. 1, p. 2650003, 2026. 10.1155/que2/6643049

[32] X. Lou, H. Zan, Z. Wang, J. Shi, and S. Zhang, "Privacy-preserving bidirectional data transmission of smart grid via semi-quantum computation: on mutual identity and message authentication," *IEEE Transactions on Dependable and Secure Computing*, vol. 22, no. 5, pp.5537–5548, May 2025. 10.1109/TDSC.2025.3568707

[33] X. Lou, and Z. Wang, "A Novel Quantum-Based Mutual Authentication and Key Agreement Scheme for Smart Grid," *IEEE Transactions on Information Forensics and Security*, vol. 21, pp. 2061–2075, 2026. 10.1109/TIFS.2026.3659003

[34] X. Lou, L. Wang, "QuanFlex-GAN: A Flexible Algorithm for Image Generation via Quantum Generative Modeling," *Quantum Machine Intelligence*, vol. 7, Art. no. 87, Sep. 2025.

[35] Q. Ma, D. Wu and X. Luo, "A review of deep learning-based power load forecasting methods," *International Journal of Network Dynamics and Intelligence*, vol. 4, no. 4, art. no. 100027, Dec. 2025.

[36] A. Melnik, M. Miasayedzenkau, D. Makaravets, et al., "Face generation and editing with stylegan: A survey". *IEEE Transactions on pattern analysis and machine intelligence*, vol. 46, no. 5, pp. 3557–3576, 2024.

[37] M. Mirza and S. Osindero, "Conditional generative adversarial nets," *arXiv preprint arXiv:1411.1784*, Nov. 2014. [Online]. Available: https://arxiv.org/abs/1411.1784

[38] J. Oldfield, C. Tzelepis, Y. Panagakis, M. A. Nicolaou, and I. Patras, "Bilinear models of parts and appearances in GANs," *IEEE Trans. Pattern Anal. Mach. Intell.*, vol. 46, no. 12, pp. 8568–8579, Dec. 2024, doi: 10.1109/TPAMI.2024.3415506.

[39] T. D. Pham, M. Kitamura and T. Tsunoyama, "Fuzzy recurrence dynamics of contrast medium extravasation in computed tomography," *International Journal of Network Dynamics and Intelligence*, vol. 4, no. 3, art. no. 100022, Sept. 2025.

[40] Z. Qu, W. Shi, and P. Tiwari, "Quantum conditional GAN based on patch method for abnormal electrocardiogram generation," *Comput. Biol. Med.*, vol. 166, Art. no. 107549, Jul. 2023.

[41] Y. Quan, S. Guo, and D. Qiao, "RCFL-GAN: Resource-constrained federated learning with GANs," in *Proc. Int. Conf. Comput. Supported Cooperative Work Design (CSCWD)*, 2024, pp. 513–518.

[42] E. Richardson, Y. Sandler, and M. Zohar, "Encoding in style: A StyleGAN encoder for image-to-image translation," in *Proc. IEEE/CVF Conf. Comput. Vis. Pattern Recognit. (CVPR)*, Nashville, TN, USA, Jun. 2021, pp. 2287–2296.

[43] A. Roy and D. Dasgupta, "A novel conditional Wasserstein deep convolutional GAN," *IEEE Trans. Artif. Intell.*, early access, 2023, doi: 10.1109/TAI.2023.3288851.

[44] M. S. Rudolph, N. B. Toussaint, A. Katabarwa, S. Johri, B. Peropadre, and A. Perdomo-Ortiz, "Generation of high-resolution handwritten digits with an ion-trap quantum computer," *Phys. Rev. X*, vol. 12, no. 3, Art. no. 031010, Jul. 2022.

[45] D. Saxena, J. Cao, J. Xu, and T. Kulshrestha, "RG-GAN: Dynamic regenerative pruning for data-efficient GANs," in *Proc. AAAI Conf. Artif. Intell.*, vol. 38, no. 5, 2024, pp. 4704–4712.

[46] B. Song, S. Zhao, L. Dang, H. Wang and L. Xu, "A survey on learning from data with label noise via deep neural networks," *Systems Science & Control Engineering*, vol. 13, no. 1, art. no. 2488120, 2025.

[47] X. Song, Y. Chen, Z.-H. Feng, G. Hu, D.-J. Yu, and X.-J. Wu, "SP-GAN: Self-growing and pruning GANs," *IEEE Trans. Neural Netw. Learn. Syst.*, vol. 32, no. 6, pp. 2458–2469, Jun. 2021.

[48] S. A. Stein, B. Baheri, D. Chen, Y. Mao, Q. Guan, A. Li, B. Fang, and S. Xu, "QUGAN: A quantum state fidelity based GAN," in *Proc. IEEE Int. Conf. Quantum Comput. Eng. (QCE)*, 2021, pp. 71–81.

[49] J. Tao, J. Wang, P. Zhang, J. Zhang, K.-L. Yung, and W. H. Ip, "LEGAN: A low-light image enhancement GAN for industrial smart-cameras," *Internet Things*, vol. 25, Art. no. 101054, 2024.

[50] S. L. Tsang, M. T. West, S. M. Erfani, and M. Usman, "Hybrid quantum-classical GAN for high-resolution image generation," *IEEE Trans. Quantum Eng.*, vol. 4, pp. 1–19, 2023.

[51] J. Wang and X. Hu, "Gated recurrent convolution neural network for OCR," *Advances Neural Inf. Process. Syst. (NeurIPS)*, vol. 30, 2017.

[52] L. Wang, C. Zhou, and X. Liu, "AEC-GAN: Adversarial error correction GANs for long time-series generation," in *Proc. AAAI Conf. Artif. Intell.*, vol. 37, no. 8, 2023, pp. 10140–10148.

[53] W. Xia, Y. Zhang, Y. Yang, J. Xue, B. Zhou, and M. Yang, "GAN inversion: A survey," *IEEE Trans. Pattern Anal. Mach. Intell.*, vol. 45, no. 3, pp. 3121–3138, Mar. 2023.

[54] Z.-P. Xu, "Characterizing arbitrary quantum networks in the NISQ era," *Phys. Rev. A*, vol. 108, no. 4, Art. no. L040201, 2023.

[55] X. Xu, and X. Lou, "User-driven cross cloud-domain authentication and key agreement scheme with quantum entanglement swapping," *International Journal of Quantum Information*, vol. 24, No.01, p. 2650003, 2026. 10.1142/S0219749926500036

[56] Y. Xue, W. Tong, F. Neri, P. Chen, T. Luo, L. Zhen, and X. Wang, "Evolutionary architecture search for GANs based on weight sharing," *IEEE Trans. Evol. Comput.*, vol. 28, no. 3, pp. 653–667, Jun. 2024.

[57] X. Yan, C. Wang and Y. Jin, "Federated bimodal graph neural networks for text-image retrieval," *International Journal of Network Dynamics and Intelligence*, vol. 4, no. 2, art. no. 100009, Jun. 2025.

[58] N. K. Yadav, S. K. Singh and S. R. Dubey, "MobileAR-GAN: MobileNet-based efficient attentive recurrent generative adversarial network for infrared-to-visual transformations". *IEEE Transactions on Instrumentation and Measurement*, vol. 71, pp. 1–9 2022.

[59] Y. Yang, K. Mu, and R. H. Deng, "Lightweight privacy-preserving GAN framework for model training and image synthesis," *IEEE Trans. Inf. Forensics Security*, vol. 17, pp. 1083–1098, 2022.

[60] Y. Zhan, R. Yang, J. You, M. Huang, W. Liu and X. Liu, "A systematic literature review on incomplete multimodal learning: techniques and challenges," *Systems Science & Control Engineering*, vol. 13, no. 1, art. no. 2467083, 2025.

[61] P. Zhang, Y. Liu, S. Lai, H. Li, and L. Jin, "Privacy-preserving biometric verification with handwritten random digit string," *IEEE Trans. Pattern Anal. Mach. Intell.*, 2025, doi: 10.1109/TPAMI.2025.3529022.

[62] D. Zhao, C. Gao, J. Li, H. Fu and D. Ding, "PID control and PI state estimation for complex networked systems: a survey," *International Journal of Systems Science*, vol. 56, no. 11, pp. 2735–2750, 2025.

[63] N. Zhou, T. Zhang, X. Xie, and J. Wu, "Hybrid quantum-classical GANs for image generation via learning discrete distribution," *Signal Process. Image Commun.*, vol. 110, Art. no. 116891, 2023.

[64] Y. Zhou, B. Hu, X. Yuan, K. Huang, Z. Yi, and G. G. Yen, "Multiobjective evolutionary GAN compression for image translation," *IEEE Trans. Evol. Comput.*, vol. 17, no. 3, pp. 798–809, 2024.

VII. Biography Section

Xiaoping Lou (Member, IEEE) is a Professor with the College of Information Science and Engineering at Hunan Normal University, Changsha, China. She has been actively engaged in research on cyberspace security, information security technologies, quantum information, and quantum computing. She received her Ph.D. degree from the School of Information Science and Engineering, Central South University, Changsha, China, in 2014. Her current research interests include quantum computation and quantum cryptography. She has led research projects supported by the National Natural Science Foundation of China and the Natural Science Foundation of Hunan Province.

Chengzeng Long (Student Member, IEEE) received the B.S. degree from the College of Information Science and Engineering, Hunan University Of Chinese Medicine, Changsha, China, in 2024, and is currently pursuing the M.S. degree at the College of Information Science and Engineering, Hunan Normal University, Changsha, China.

Linghui Wang (Student Member, IEEE) received the B.S. degree from the College of Information Science and Engineering, Hunan University of Arts and Science, Changde, China, in 2022, and the M.S. degree from the College of Information Science and Engineering, Hunan Normal University, Changsha, China, in 2025.

Zidong Wang (Fellow, IEEE) received the B.Sc. degree in mathematics in 1986 from Suzhou University, Suzhou, China, and the M.Sc. degree in applied mathematics in 1990 and the Ph.D. degree in electrical engineering in 1994, both from Nanjing University of Science and Technology, Nanjing, China.

He is currently Professor of Dynamical Systems and Computing in the Department of Computer Science, Brunel University London, U.K. From 1990 to 2002, he held teaching and research appointments in universities in China, Germany and the UK. Prof. Wang's research interests include dynamical systems, signal processing, bioinformatics, control theory and applications. He has published a number of papers in international journals. He is a holder of the Alexander von Humboldt Research Fellowship of Germany, the JSPS Research Fellowship of Japan, William Mong Visiting Research Fellowship of Hong Kong.

Prof. Wang serves (or has served) as the Editor-in-Chief for *International Journal of Systems Science*, the Editor-in-Chief for *Neurocomputing*, the Editor-in-Chief for *Systems Science & Control Engineering*, and an Associate Editor for 12 international journals including *IEEE Transactions on Automatic Control*, *IEEE Transactions on Control Systems Technology*, *IEEE Transactions on Neural Networks*, *IEEE Transactions on Signal Processing*, and *IEEE Transactions on Systems, Man, and Cybernetics-Part C*. He is a Member of the Academia Europaea, a Member of the European Academy of Sciences and Arts, an Academician of the International Academy for Systems and Cybernetic Sciences, a Fellow of the IEEE, a Fellow of the Royal Statistical Society, and a member of program committee for many international conferences.